Simulation Study of a Monolithic III-V/Si V-Groove Carrier Depletion Optical Phase Shifter

Sanghyeon Kim, *Member, IEEE*, Younghyun Kim, *Member, IEEE*, Yoojin Ban, Marianna Pantouvaki, and Joris Van Campenhout

***Abstract*— In this paper, we propose a new carrier depletion-type hybrid III-V/Si optical phase shifter using a n-III-V/p-Si hetero-junction, which can be fabricated with direct epitaxial growth of III-V semiconductors on Si. We numerically analyzed the performance of the III-V/Si hybrid optical phase shifter by comparing the performance in reverse bias operation with that of pure Si or III-V p-n optical phase shifters. The hybrid III-V/Si optical phase shifter showed improved modulation efficiency and lower optical loss compared to pure Si and III-V p-n optical phase shifters, owing to the large electron-induced refractive index change of III-V compound semiconductors, while avoiding the large hole-induced optical loss of III-V compound semiconductor. The simulation study suggests the feasibility of a very low voltage-length product ($V_\pi L$) of 0.07 V · cm, a low insertion loss (α) of 16 dB/cm, and a very low $\alpha\ V_\pi L$ product close to 1 V · dB at 1.31 μ m, which is 10x lower than for Si p-n optical phase shifters.**

***Index Terms*— Optical phase shifter, optical modulation, heterogeneous integration, III-V on Si, hybrid integration.**

I. Introduction

OPTICAL phase shifters are fundamental building blocks for Si photonic integrated circuits [1]–[3]. Implemented in an interferometer system such as a Mach-Zehnder interferometer or ring resonator, it provides optical amplitude modulation and switching. Generally, Si-based optical phase shifters use the free-carrier plasma effects of Si. Modulating the carrier density results in the change of the refractive index, which changes the phase of the light. P-n junctions, p-i-n junctions, and semiconductor/insulator/semiconductor junctions have been used to realize the carrier density modulation [4]–[7]. However, inherently weak free-carrier effects of Si fundamentally limit the performance of the optical phase shifter in terms of device footprint, optical loss, modulation bandwidth, etc. To mitigate these limitations, many researchers have devoted lots of efforts in very recent years to material and structure engineering [8]–[15]. Among them, one of the key breakthroughs in recent developments is the introduction of new materials such as III-V compound semiconductors, which have superior free-carrier effects due to lower effective mass and higher mobility than those of Si [16]–[23]. Recent reports from many groups using wafer bonding-based approaches demonstrated very low voltage-length product ($V_\pi L$) as small as 0.05 V · cm at 20 dB/cm loss, which cannot be achieved in Si-based optical phase shifter [19]–[22]. Although those demonstrations clearly showed the feasibility of III-V/Si hybrid integration for the optical phase shifter, the processing steps for the bonding thin films as well as III-V contact metallization add substantial complexity and manufacturability challenges in present CMOS facilities.

Here, therefore, we propose a new carrier depletion-type hybrid III-V/Si optical phase shifter based on the hetero-epitaxy technique [16], which relaxes process challenges and may open a route to implementation in CMOS processing lines. Furthermore, it can further enhance the performance of the optical phase shifter by enhancing the Franz-Keldysh effect [17]. Through systematic computer-aided design (TCAD) simulations, we carefully investigated the performance potential of several hybrid device structures and compared the performance with Si-based p-n junctions and III-V-based p-n junctions. The results show very high modulation efficiency ($V_\pi L$ of 0.07 $V \cdot$ cm), a low optical loss (α) of 16 dB/cm, and a very low $\alpha V_\pi L$ product close to 1 V · dB, clearly indicating the potential of the proposed phase shifter.

II. Hybrid Modulator Modeling

To model the hybrid modulator, we first numerically calculated the change of the refractive index (Δn) and absorption coefficient ($\Delta\alpha$) for various III-V compound semiconductors by the change of the carrier density.

A. Numerical Calculation of the Change in Refractive Index and Absorption Coefficient

The plasma dispersion effect and free-carrier absorption in semiconductors are described as equation 1, where e is the elementary charge, ε_0 is the permittivity in vacuum, c is the speed of light in vacuum, λ is the wavelength, n is the unperturbed refractive index, m^*ce and m^*ch are the conductivity effective masses of electrons and holes, and μ_e and μ_h are the mobilities of electrons and holes, respectively.

$$\Delta n = -\frac{e^2\lambda^2}{8\pi^2 c^2 \varepsilon_0 n}\left(\frac{\Delta N_e}{m^*_{ce}} + \frac{\Delta N_{\mathrm{h}}}{m^*_{\mathrm{ch}}}\right) \quad (1)$$

Manuscript received November 4, 2019; revised December 28, 2019; accepted January 27, 2020. Date of publication February 5, 2020; date of current version February 12, 2020. This work was supported in part by the IMEC's industry affiliation Research and Development program on Optical I/O. *(Corresponding author: Younghyun Kim.)*

Sanghyeon Kim was with the IMEC, B-3001 Leuven, Belgium. He is now with the School of Electrical Engineering, Korea Advanced Institute of Science and Technology (KAIST), Daejeon 34141, South Korea (e-mail: shkim.ee@kaist.ac.kr).

Younghyun Kim, Yoojin Ban, Marianna Pantouvaki, and Joris Van Campenhout are with the IMEC, B-3001 Leuven, Belgium (e-mail: younghyun.kim@imec.be; yoojin.ban@imec.be; marianna.pantouvaki@imec.be; joris.vancampenhout@imec.be).

Color versions of one or more of the figures in this article are available online at http://ieeexplore.ieee.org.

Digital Object Identifier 10.1109/JQE.2020.2971764

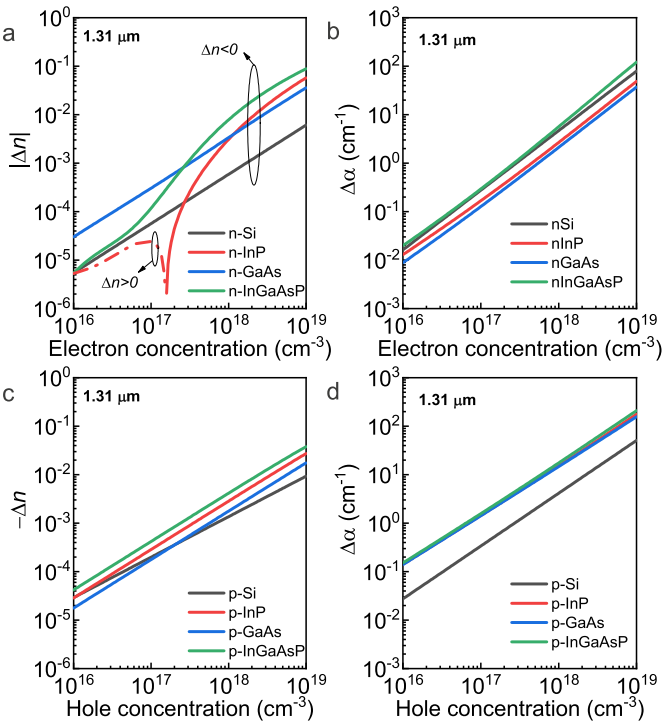

Fig. 1. Δn and $\Delta\alpha$ characteristics in various III-Vs (InP, GaAs, InGaAsP) and Si as a function of electron and hole concentration at 1.31 μm.

$$\Delta\alpha = \frac{e^3\lambda^2}{4\pi^2 c^3 \varepsilon_0 n}\left(\frac{\Delta N_e}{m^*_{ce}\mu_e} + \frac{\Delta N_h}{m^*_{ch}\mu_h}\right). \tag{2}$$

As shown in equation (1) and (2), an effective mass (both electron and hole) plays an important role in the plasma dispersion effect, indicating that III-V compound semiconductors provide larger effects than Si. The band-filling effect and bandgap shrinkage effect should be taken account to estimate Δn in III-V compound semiconductors [24]–[26]. For hole, the inter-valence band absorption is known to be the main contributor for the free-carrier absorption in p-type III-V compound semiconductor, thereby need to be considered [25], [26].

Therefore, by taking account these effects, we numerically calculated the Δn and $\Delta\alpha$ in Si and various III-V such as InP, GaAs, $In_{0.82}Ga_{0.18}As_{0.4}P_{0.6}$ (InGaAsP) at 1.31 μm as a function of electron and hole densities. Here, mobility degradation due to the impurity scattering with increasing the doping concentration was also taken account for this calculation [27]. Fig. 1 shows the carrier-induced Δn and $\Delta\alpha$ of Si, InP, GaAs, and InGaAsP. As shown in Fig. 1(a), electron-induced Δn is much higher in III-V material than that of Si due to smaller effective mass. The absorption coefficients of III-V materials are comparable or even smaller $\Delta\alpha$ in Fig. 1(b). Despite of smaller effective mass, higher mobility values compensated the increase of $\Delta\alpha$. It is one of the key benefits of III-V compound semiconductor compared to Si. These results indicate the use of electron-induced Δn of III-V compound semiconductor in the optical phase shifter would be very beneficial to increase the efficiency.

On the other hand, hole-induced Δn of III-V compound semiconductor seems to be also beneficial in terms of efficient phase change of the light compared to Si. However, at the same time, considerably high optical loss ($\Delta\alpha$) is expected due to the inter-valence band absorption when the p-type III-V compound semiconductor is used as an optical phase shifter, as shown in Fig. 1(d).

Therefore, the appropriate material combination will be an important point to achieve the efficient optical phase shifter.

B. Numerical Analysis of Optical Phase Shifters

To address the impact of free-carrier effects in III-V compound semiconductors and Si and systematically investigate the feasibility of the newly proposed structure in this work, we quantitatively studied four different device structures in Fig. 2. Fig. 2(a) shows the conventional Si optical phase shifter using Si pn junction. Fig. 2(b) shows the all III-V optical phase shifter using InP pn junction. Figs. 2(c) and 2(d) show III-V/Si hybrid optical phase shifter using hybrid hetero-junction with planar and V-shaped structures with a Si waveguide (WG). For all structures, we assumed a WG width of 475 nm and a WG height of 210 nm, which satisfy a single mode condition. Contact layers for p+Si and n+Si were placed on the lateral side of WG with an offset of 300 nm from the edge of the WG. Ohmic contact was assumed in metal/semiconductor contact in the simulation. Other detailed dimensions and doping concentration (acceptor concentration, N_A and donor concentration, N_D) are shown in Fig. 2. Here, we used the constant doping profile in each region to simplify the simulation.

Modeling can be divided into two parts. First, we achieved carrier distribution at a given bias condition using TCAD simulation. Fig. 3(a) shows the cross-sectional potential energy distribution at the center region in the hybrid optical phase shifter shown in Fig. 2(d) with two different bias conditions of 0 V and −1.5 V (reverse bias condition). With reverse bias, n-InP/p-Si junction is depleted, resulting in a change of the carrier distribution near the junction interface. Also, it can be clearly seen in the 2D cross-sectional image in Fig. 3(b). Then, carrier distributions were imported into optical mode solver and the optical mode was calculated considering the carrier-induced Δn and $\Delta\alpha$ both in Si and III-V as shown in Fig. 3(c). With this method, we estimated $V_\pi L$ and α of the devices and discussed the potential performances of the devices.

III. Discussion

A. Optical Phase Shifters With Si pn Junction and InP pn Junction

First, we investigated the optical phase shifter with pn junction of a single material. Figs. 4(a), 4(b), and 4(c) show the change of effective refractive index (Δn_{eff}), $V_\pi L$, and α of the optical phase shifter with Si pn and InP pn junctions as a function of applied bias voltages, respectively. Here, N_A and N_D were assumed to $5 \times 10^{17}\text{cm}^{-3}$. All parameters were extracted from the fundamental TE mode at 1.31 μm, as shown in the inset of Fig. 4(c). The Δn_{eff} increases with increasing a bias voltage for both Si and InP due to increased depletion region at the junction interface. The Δn_{eff} of the

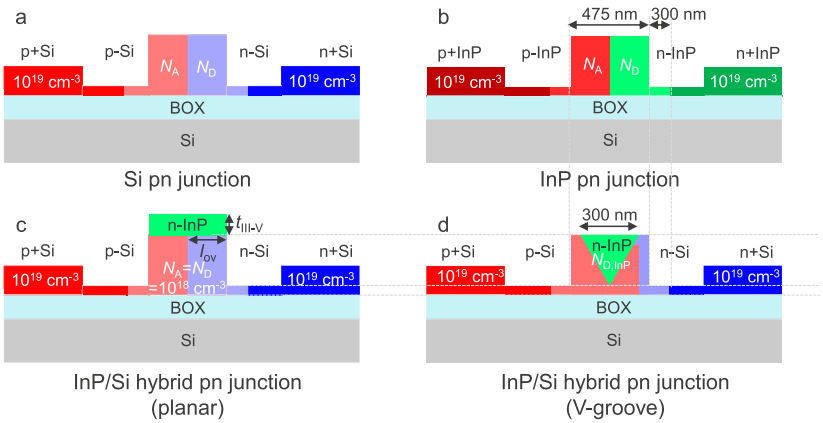

Fig. 2. Cross-sectional structure of (a) Si and (b) InP pn optical phase shifter and InP/Si hybrid (c) plane and (d) V-groove optical phase shifter. Device dimensions are also shown in the figure.

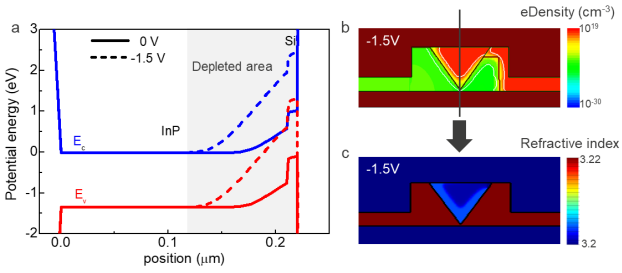

Fig. 3. (a) Band diagram at the n-InP/p-Si interface with and without reverse bias. (b) Electron density and (c) refractive index distribution of InP/Si hybrid waveguide with reverse bias.

optical phase shifter with InP pn junction is higher than that with Si pn junction. It would be highly related to enhanced electron-induced free-carrier effect, as shown in Fig. 1, resulting in much lower $V_\pi L$ at whole range of the applied voltage in Fig. 4(b). Meanwhile, InP optical phase shifter shows higher α than Si optical phase shifter due to large inter-valence band absorption, as discussed in section II. Therefore, it makes a fundamental trade-off between efficiency ($V_\pi L$) and α, whereas the performance can be further improved by material engineering using InGaAsP, etc. [14]. We also investigated the impact of the N_A/N_D on the performance in the Si and InP optical phase shifter in Figs. 4(d), 4(e), and 4(f). Similar trends were found even with different doping concentrations. Lower $V_\pi L$, but considerably higher α were obtained in InP optical phase shifter over Si optical phase shifter, whereas $\alpha V_\pi L$ shows still lower values. Therefore, it is quite important to maximize the electron-induced Δn, while minimizing the hole-induced $\Delta\alpha$ of III-V materials in optical phase shifter to optimize performances between $V_\pi L$ and α. Hybridization of Si and III-V would be one of the promising directions to realize this.

B. III-V/Si Hybrid Planar Optical Phase Shifter

To take advantage of the large electron-induced Δn of III-V materials, not but the large increase of hole-induced $\Delta\alpha$ of III-V materials, we have considered the Si/III-V hybrid optical phase shifter as shown in Figs. 2(c) and 2(d). First, we considered the integration of a planar thin n-type III-V film by thin film growth on top of the Si pn WG (Fig. 2(c)) as the similar structure has been demonstrated to improve modulation efficiency by SiGe [12]. Since grown n-III-V and n-Si is electrically conductive, the carrier depletion at the interface between n-III-V and p-Si can be expected. Therefore, an electron-induced Δn of III-V materials can be used in the phase shifter with this hybrid structure while avoiding a hole-induced effect of III-V materials. Geometric factors would have a positive impact on the performance because the optical confinement factor in the depletion layer at n-III-V/p-Si interface can be changed depending on the device geometry. Thus, we investigated the $V_\pi L$ and α of III-V/Si hybrid optical phase shifter with various overlap length (l_{ov}) between n-Si and n-III-V and the thickness of the n-III-V layer (t_{III-V}). Fig. 5 shows the $V_\pi L$ and α in InP/Si hybrid optical phase shifters as a function of t_{III-V}, and as a parameter of l_{ov}.

First, with the thin III-V layer thinner than 50 nm, the estimated $V_\pi L$ is positioned slightly above and somewhat between Si pn optical phase shifter and InP pn optical phase shifter depending on l_{ov} because the optical mode overlap with junction interface changes with a change of l_{ov} and t_{III-V}, as shown in Fig 5(a). With a relatively thick III-V layer, $V_\pi L$ decreases with an increase of t_{III-V}. It would be attributed to the increase of optical mode overlap with the III-V/Si depletion region. Meanwhile, the case of 380-nml_{ov} showed quite large $V_\pi L$ even larger than Si optical phase shifter due to the small contribution of InP on $V_\pi L$ due to the small volumetric portion of n-InP/p-Si junction. Here, one important feature is that decreased $V_\pi L$ value saturates at $V_\pi L$ of InP pn optical phase shifter because the contribution of electron-induced Δn of InP is a dominant factor to decide the efficiency in this structure. On the other hand, the α of III-V/Si hybrid optical phase shifter was lower than that of InP and Si pn optical phase shifter. It would be attributed to the significant reduction of the hole-induced α by eliminating p-InP in the device structure.

Above results strongly suggest that n-InP/p-Si hybrid optical phase shifter can provide comparable $V_\pi L$ with InP pn optical phase shifter with the reduced optical loss even lower than Si pn optical phase shifter. However, to achieve this benefit, relatively thick III-V material is needed ($t_{III-V} > 50$ nm),

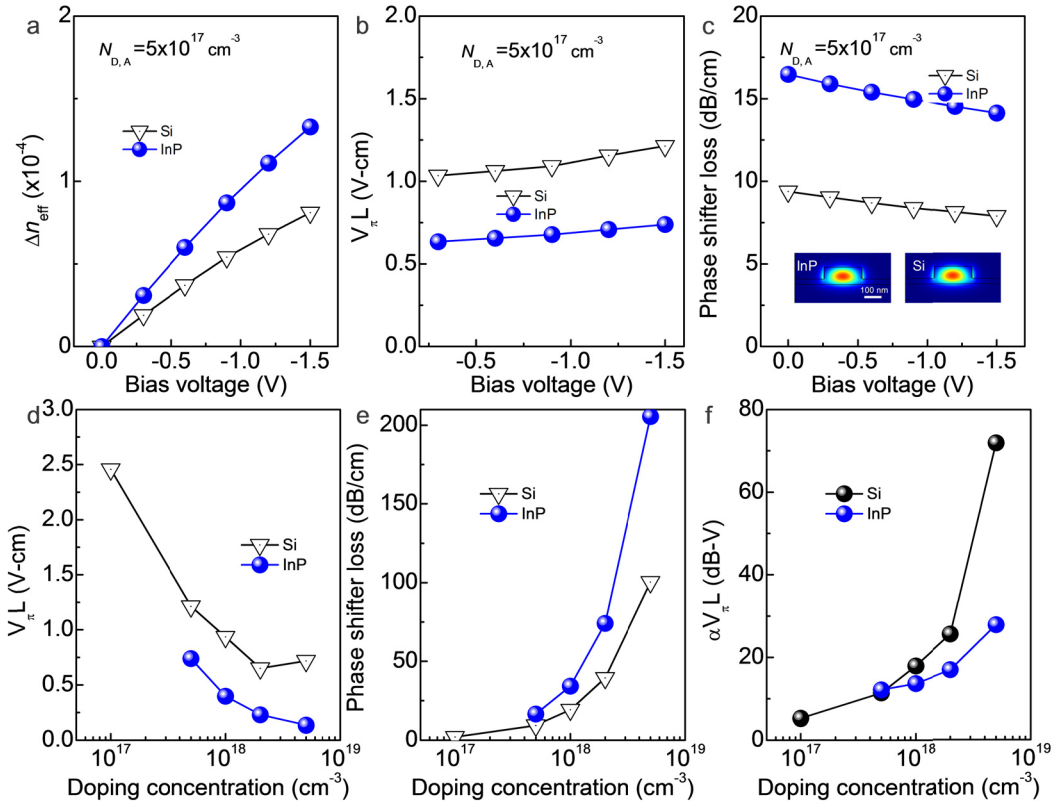

Fig. 4. (a) Δn_{eff}, (b) $V_\pi L$, and (c) α characteristics of InP and Si pn optical phase shifter as a function of bias voltage. The (d) $V_\pi L$, (e) α, and (f) $\alpha V_\pi L$ characteristics of InP and Si pn optical phase shifter as a function of doping concentration of semiconductor layer.

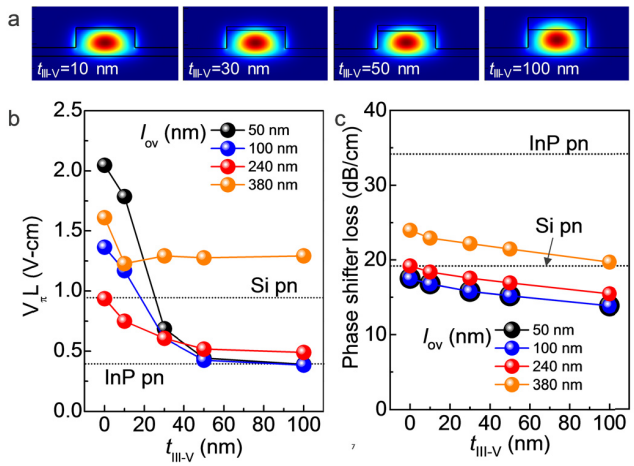

Fig. 5. The $V_\pi L$ and optical loss characteristics of InP/Si hybrid planar optical phase shifter.

whereas epitaxial growth of III-V single crystal directly on Si is quite challenging in such thickness range due to the large lattice mismatch between III-V and Si [28]–[31].

C. III-V/Si Hybrid V-Shape Optical Phase Shifter

As shown in Section B, hybrid optical phase shifter potentially provides improved performance than typical Si and III-V pn optical phase shifters. However, the limited optical mode confinement in III-V material and the epitaxial film growth would restrict the performance enhancement in hybrid planar optical phase shifters.

On the other hand, a relatively high-quality III-V film can be grown on V-groove of a Si substrate. The previous works reported the demonstration of III-V laser using InP directly grown on Si V-groove, showing the great potential of this growth approach for photonic devices [16]. Therefore, we have proposed the III-V/Si optical phase shifter [32] and in this study, simulated the InP/Si hybrid optical phase shifter assuming epitaxially grown InP on V-groove of Si waveguide, as shown in Fig. 2(d). Not only for the realistic implementation in terms of the epitaxial growth, this structure can also provide enhanced optical confinement in n-InP/p-Si heterojunction, leading to large performance improvement.

Figs. 6 (a) and 6 (b) shows the Δn_{eff} and optical loss of InP/Si hybrid V-shape optical phase shifter as a function of an applied bias voltage. Here, the doping concentration of n-InP ($N_{\text{D,InP}}$) was varied from 5×10^{17} to 5×10^{18} cm^{-3} and N_{A}, N_{D} of the Si WG was fixed to 5×10^{17} cm^{-3}. Clear optical mode confinement in the InP layer was observed in the inset of Fig. 6(a).

With an increase of the applied bias voltage, Δn_{eff} increases and α decreases due to the carrier depletion at the n-InP/p-Si interface, as shown in Fig. 3. High N_{D} in n-InP leads to higher Δn_{eff} and α due to large free-carrier effects. Corresponding $V_\pi L$ and $\alpha V_\pi L$ were estimated in Figs. 6(c) and 6(d). Low $V_\pi L$ ranging 0.05 – 0.2 V·cm was obtained with N_{D} in n-InP of the order of 10^{18} cm^{-3}. Obviously, high N_{D} leads to

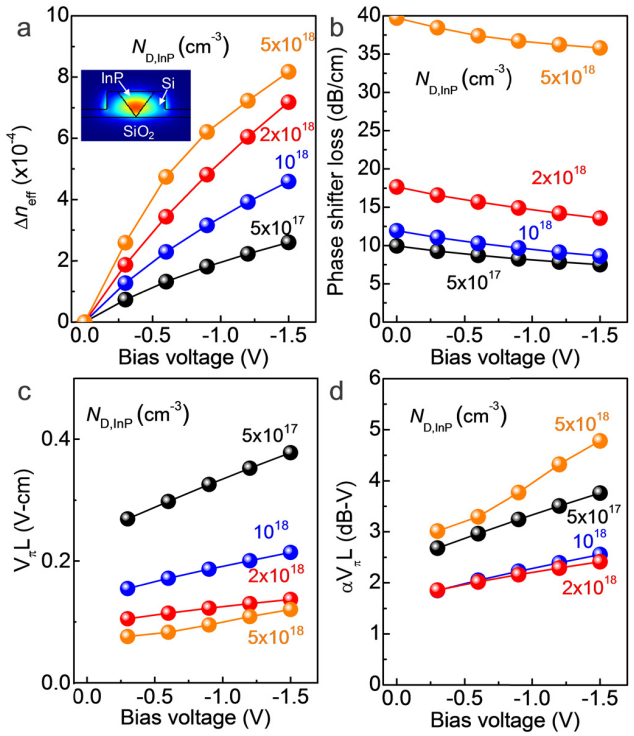

Fig. 6. (a) Δn_{eff}, (b) phase shifter loss, (c) $V_\pi L$, and (d) $\alpha V_\pi L$ of InP/Si hybrid V-shape optical phase shifter as a function of applied reverse bias voltage with variable N_{D} values in n-InP.

lower $V_\pi L$, and the lowest $V_\pi L$ was obtained with N_{D} of 5×10^{18} cm^{-3} according to the increased Δn_{eff}. However, the lowest $\alpha V_\pi L$, which is the figure-of-merit considering the optical loss as well as modulation efficiency simultaneously, was obtained with N_{D} of 2×10^{18} cm^{-3} because too high N_{D} cause high optical loss of the optical phase shifter. Therefore, the appropriate choice of N_{D} in the InP layer will be important for target speculations and driving conditions such as extinction ratio, insertion loss, and phase-shifter length, driving voltages, etc. respectively. Above all, realistic implementation is expected with this structure because it potentially provides high-quality III-V film on Si WG.

D. Impact of TDD in III-V Epitaxial Layer on III-V/Si Hybrid Optical Phase Shifter

One possible concern of our proposed hybrid optical phase shifter for real implementation would be the defect generation during the epitaxial growth of III-V material on Si [28]–[31]. Therefore, we investigated the impact of the threading dislocation density (TDD) on the performance in III-V/Si hybrid V-shape optical phase shifter. TDD in III-V materials would increase the dark current and it will reduce the electric field penetration at III-V/Si interface, possibly resulting in performance degradation in optical phase shifters.

To consider the TDD in TCAD simulation, we changed SRH recombination lifetime in InP layer, which is represented by the following equation, where τ_{SRH}, $\tau_{\text{SRH,w/oTDD}}$, τ_{TDD}, and D are modified SRH lifetime due to TD, SRH lifetime without TD, the lifetime for recombination through TD, and carrier

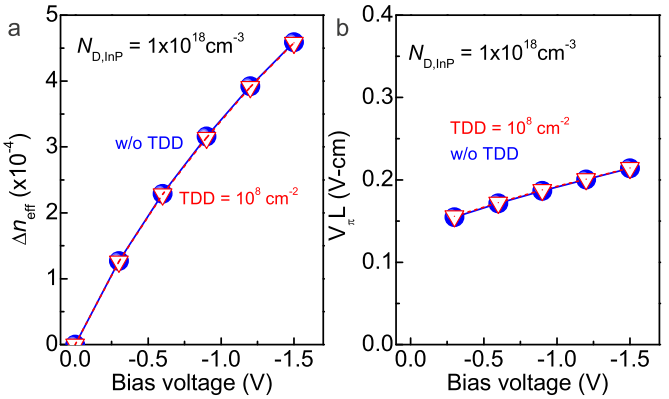

Fig. 7. (a) Δn_{eff} and (b) $V_\pi L$ of InP/Si hybrid V-shape optical phase shifter with and without TDD of 10^8 cm^{-2} as a function of applied bias voltage.

diffusion coefficient, respectively [31].

$$\frac{1}{\tau_{SRH}} = \frac{1}{\tau_{SRH,w/oTDD}} + \frac{1}{\tau_{TDD}}$$
$$\tau_{TDD} = \frac{4}{\pi^3 D \cdot TDD}. \quad (3)$$

Here, we assumed $\tau_{\text{SRH,w/oTDD}}$ and D for electron/hole as 5 ns /2.5 ns and 78 cm^2/s/7.1 cm^2/s, respectively.

Fig. 7 shows the Δn_{eff} of optical mode and $V_\pi L$ of InP/Si hybrid V-shape optical phase shifter with and without TDD as a function of applied reverse bias. Here, N_{D} in InP was assumed to 10^{18} cm^{-3} and TDD level was assumed to 10^8 cm^{-2}, which is comparable value in the previous report [33]. Even with such a high TDD level, Δn_{eff} exactly follows the data without TDD (slightly smaller), indicating the n-InP/p-Si interface with TDD in InP can show sufficient surface depletion behavior. Defects may increase the electron density in InP grown on Si, but the density would be not so high level, which can impact on the performance. It is quite difficult to make a statement on InP on Si because direct measurement of the carrier density has not been carried out. Nevertheless, we believe that interface control and material control during the growth will promise low intrinsic N_{D} level because a typical N_{D} level of III-V (InAs or GaSb) on Si V-groove was around 10^{17} cm^{-3} or even lower [34]. Furthermore, unintentional doping due to the defects can be annihilated by hydrogen termination [35], [36].

On the other hand, TDD would degrade the mobility in the n-InP layer, which will impact on the optical loss. Therefore, the impact on the optical loss is still questionable, and the measurement of actual mobility of the epitaxially grown InP layer on Si will be important to address the full potential of our proposed device.

IV. Benchmarking

First, we compared the performance of the optical phase shifter for different device structures such as Si pn optical phase shifters, InP pn optical phase shifters, InP/Si hybrid planar optical phase shifters, and InP/Si hybrid V-shape optical phase shifters. Since the doping concentration of semiconductors in an optical phase shifter impact on both $V_\pi L$ and α,

TABLE I

BENCHMARK OF THE PERFORMANCE MATRIX FOR OPTICAL MODULATORS WITH VARIOUS DEVICE STRUCTURES

Reference	[4] G. T. Reed (2014)	[6] M. Webster (2015)	[9] H. Yu (2012)	[10] Z. Yong (2017)	[12] J. Fujikata (2018)	[19] J. –H. Han (2017)	[20] T. Hiraki (2017)	This work (sim.)
Junction type	Si lateral pn	Poly-Si/SiO_2/Si	Si Inter-digitated	U-shaped pn	p-SiGe, Si/n-Si	n-III-V/ Al_2O_3/p-Si	n-III-V/ SiO_2/p-Si	n-III-V/ p-Si
Wavelength (nm)	1550	1310	1550	1310	1310	1550	1550	1310
$V_\pi L$ (V·cm)	1.4 – 1.9	0.2	1.12	0.26-0.46	0.81	0.047	0.09	0.07
α (dB/cm)	40	65	25	12.5	30-40	19.4	26	16
$\alpha V_\pi L$ (dB·V)		13	28	3.25-5.75		0.91	2.34	1
Junction capacitance (pF/mm)	-(52 Gbit/s demonstrated)	1.25 – 5 at 1.2 – 2.2 V	0.8 – 1.59 at 1 – 6 V	0.3 – 2.2 at 1 – 5 V	0.36 – 0.66 at 0 – 3 V	6 at 1.5 V	- (32 Gbit/s demonstrated)	0.9-1.2 at 1.5 V

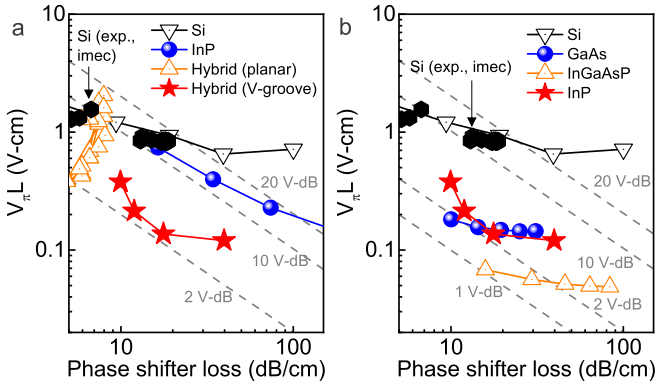

Fig. 8. (a) $V_\pi L$ - α relationship in various optical phase shifter structures (b) $V_\pi L$ - α relationship of III-V/Si hybrid V-shape optical phase shifter with various III-V materials such as InP, GaAs, InGaAsP.

which are typically in the trade-off relationship, we plotted $V_\pi L$ value as a function of α for the benchmark in Fig. 8(a). We also plotted the experimental data of a Si pn optical phase shifter with the closed black hexagon. First, experimental data were well-matched with our simulated data, validating our proper model calibration. As discussed in Section III-A, the InP pn optical phase shifter shows smaller $V_\pi L$ but larger α than the Si pn optical phase shifter in between 10 dB·V and 20 dB·V lines. On the other hand, the InP/Si hybrid optical phase shifter shows noticeable improvement reaching to 2 dB·V lines, indicating hybridization is crucially important to enhance the device performance breaking the $V_\pi L$ - α trade-off line of the conventional Si pn optical phase shifter. Here, it should be noted that the apparent opposite trend of $V_\pi L$ - α in the hybrid planar optical phase shifter would be because the optical mode overlaps with III-V/Si junction in the device impacts on the performance as shown in Fig. 5. Furthermore, it should be emphasized that the InP/Si hybrid optical phase shifter does not have a physical metal contact for InP, which is the remarkable advantages over wafer bonding-based hybrid optical phase shifter in terms of process integration.

In terms of the active materials, the proposed device structure does not limit the material species if the epitaxial growth is possible. We simulated the InP/Si hybrid optical phase shifter in Section II and III, but various III-V materials are applicable instead of InP in the III-V/Si hybrid optical phase shifter. Therefore, to compare the potential performance for each material, we additionally simulated III-V/Si hybrid V-shape optical phase shifters using GaAs and InGaAsP. The $V_\pi L$ - α relationship of the hybrid optical phase shifter with various III-V materials are shown in Fig. 8(b). Since InGaAsP has the largest free-electron effect, InGaAsP/Si hybrid optical phase shifter shows the highest performance enabling $\alpha V_\pi L$ product near 1 V·dB line. Here, the predicted optical absorption levels may be negatively affected by lower mobility values obtained in III-V directly grown on Si. Such an impact is expected if threading dislocation densities in III-V would substantially exceed 10^8 – 10^9 cm^{-2}.

Table. I shows the benchmark of the performance matrix such as $V_\pi L$, α, $\alpha V_\pi L$, and junction capacitance for optical modulators with various device structures [4], [6], [9], [10], [12], [19], [20]. Here, we investigated junction capacitance because this is a very important parameter to estimate the bandwidth of the devices, whereas the present study has not focused on bandwidth performance. Performances of Si-based modulators are significantly affected by junction geometry (lateral pn, SIS, Inter-digitated pn, U-shaped pn) and figure-of-merits are in the trade-off relationship. For example, $V_\pi L$ and junction capacitance show the trade-off because increasing junction area increases the modulation efficiency, but increase capacitance at the same time. This benchmark directly shows the fundamental limitation of Si, which can be mitigated by introducing SiGe or III-V materials [12], [19], [20]. Remarkably, our proposed new structure of n-III-V/p-Si hetero-junction shows high potential to achieve low all figure-of-merits of $V_\pi L$, α, $\alpha V_\pi L$, and junction capacitance. This would be attributed to the geometrical advantages of V-groove like U-shaped Si pn junction [10] and material advantages using the superior free-electron effect of III-V on p-Si.

Through the above benchmarks, we believe that the III-V/Si hybrid V-shape optical phase shifter has high potential as a promising technology to provide highly efficient and low loss light modulation in Si photonic integrated circuits.

Finally, the fabrication challenges in the proposed structure would remain the epitaxial growth of III-V layers on Si

because another process step is not new but very conventional. Even though we already reported several related demonstrations [16], [18], the quality of the epitaxial films would be very important for the high performance of the devices.

V. Conclusion

In this study, we systematically investigated the performance of various types of optical phase shifters including the typical Si p-n optical phase shifter, the InP p-n optical phase shifter, and InP/Si hybrid optical phase shifters (planar and V-shape) by TCAD simulation. Hybridization of n-InP and p-Si in the optical phase shifter was shown to be a very efficient way to increase the performance by leveraging the large electron-induced Δn of III-V materials, but avoiding large hole-induced α of III-V materials. In order to realize the projected performance gains, we proposed a hybrid waveguide carrier depletion phase shifter structure consisting of a hetero-interface with n-III-V directly grown in a V-groove on a p-Si base. The simulations showed very low $V_\pi L$ of 0.07 V$\cdot$cm, a low optical loss α of 16 dB/cm and a very low $\alpha V_\pi L$ product close to 1 V$\cdot$dB at 1.31 μm, which cannot be achieved by typical Si p-n optical phase shifters.

References

[1] M. Pantouvaki *et al.*, "Active components for 50 Gb/s NRZ-OOK optical interconnects in a silicon photonics platform," *J. Lightw. Technol.*, vol. 35, no. 4, pp. 631–638, Feb. 2017, doi: 10.1109/jlt.2016.2604839.

[2] G. T. Reed, G. Mashanovich, F. Y. Gardes, and D. J. Thomson, "Silicon optical modulators," *Nature Photon.*, vol. 4, pp. 518–526, Jul. 2010, doi: 10.1038/nphoton.2010.179.

[3] P. Dong, L. Chen, and Y.-K. Chen, "High-speed low-voltage single-drive push-pull silicon Mach-Zehnder modulators," *Opt. Express*, vol. 20, no. 6, pp. 6163–6169, Mar. 2012, doi: 10.1364/oe.20.006163.

[4] G. T. Reed *et al.*, "High-speed carrier-depletion silicon Mach-Zehnder optical modulators with lateral PN junctions," *Front. Phys.*, vol. 2, Dec. 2014, Art. no. 77, doi: 10.3389/fphy.2014.00077.

[5] S. Akiyama and T. Usuki, "High-speed and efficient silicon modulator based on forward-biased pin diodes," *Front. Phys.*, vol. 2, Nov. 2014, Art. no. 65, doi: 10.3389/fphy.2014.00065.

[6] M. Webster, C. Appel, P. Gothoskar, S. Sunder, B. Dama, and K. Shastri, "Silicon photonic modulator based on a MOS-capacitor and a CMOS driver," in *Proc. IEEE Compound Semicond. Integr. Circuit Symp. (CSICS)*, Oct. 2014, pp. 1–4, doi: 10.1109/csics.2014.6978577.

[7] A. Liu *et al.*, "A high-speed silicon optical modulator based on a metal-oxide-semiconductor capacitor," *Nature*, vol. 427, pp. 615–618, Feb. 2004, doi: 10.1038/nature02310.

[8] Z.-Y. Li *et al.*, "Silicon waveguide modulator based on carrier depletion in periodically interleaved PN junctions," *Opt. Express*, vol. 17, no. 18, pp. 15947–15958, Aug. 2009, doi: 10.1364/oe.17.015947.

[9] H. Yu *et al.*, "Performance tradeoff between lateral and interdigitated doping patterns for high speed carrier-depletion based silicon modulators," *Opt. Express*, vol. 20, no. 12, pp. 12926–12938, Jun. 2012, doi: 10.1364/oe.20.012926.

[10] Z. Yong *et al.*, "U-shaped PN junctions for efficient silicon Mach-Zehnder and microring modulators in the O-band," *Opt. Express*, vol. 25, no. 7, pp. 8425–8439, Apr. 2017, doi: 10.1364/oe.25.008425.

[11] Y. Kim, M. Takenaka, T. Osada, M. Hata, and S. Takagi, "Strain-induced enhancement of plasma dispersion effect and free-carrier absorption in SiGe optical modulators," *Sci. Rep.*, vol. 4, Apr. 2014, Art. no. 4683, doi: 10.1038/srep04683.

[12] J. Fujikata *et al.*, "High-speed and highly efficient Si optical modulator with strained SiGe layer," *Appl. Phys. Express*, vol. 11, no. 3, Mar. 2018, Art. no. 032201, doi: 10.7567/apex.11.032201.

[13] J.-H. Han, P. Bidenko, J. Song, and S. Kim, "Feasibility study on negative capacitance SIS phase shifter for low-power optical phase modulation," in *Proc. Int. Conf. Group IV Photon.*, Cancun, Mexico, Aug. 2018, pp. 39–40, Paper P12, doi: 10.1109/GROUP4.2018.8478706.

[14] N. Sekine, J.-H. Han, S. Takagi, and M. Takenaka, "Numerical analysis of carrier-depletion InGaAsP optical modulator with lateral PN junction formed on III-V-on-insulator wafer," *Jpn. J. Appl. Phys.*, vol. 56, no. 4S, Mar. 2017, Art. no. 04CH09, doi: 10.7567/JJAP.56.04CH09.

[15] S. Kim, J.-H. Han, W. J. Choi, J. D. Song, and H.-J. Kim, "Functionalized bonding materials and interfaces for heterogeneously layer-stacked applications," *J. Korean Phys. Soc.*, vol. 74, no. 2, pp. 82–87, Jan. 2019, doi: 10.3938/jkps.74.82.

[16] Z. Wang *et al.*, "Room-temperature InP distributed feedback laser array directly grown on silicon," *Nature Photon.*, vol. 9, no. 12, pp. 837–842, Dec. 2015, doi: 10.1038/nphoton.2015.199.

[17] Q. Li, C. P. Ho, S. Takagi, and M. Takenaka, "Efficient optical modulator by reverse-biased III-V/Si hybrid MOS capacitor based on FK effect and carrier depletion," in *Proc. Opt. Fiber Commun. Conf. (OFC)*, San Diego, CA, USA, 2019, pp. 3–7

[18] Y. Shi *et al.*, "Optical pumped InGaAs/GaAs nano-ridge laser epitaxially grown on a standard 300-mm Si wafer," *Optica*, vol. 4, no. 12, p. 1468, Dec. 2017, doi: 10.1364/optica.4.001468.

[19] J.-H. Han, F. Boeuf, J. Fujikata, S. Takahashi, S. Takagi, and M. Takenaka, "Efficient low-loss InGaAsP/Si hybrid MOS optical modulator," *Nature Photon*, vol. 11, no. 8, pp. 486–490, Aug. 2017, doi: 10.1038/nphoton.2017.122.

[20] T. Hiraki *et al.*, "Heterogeneously integrated III-V/Si MOS capacitor Mach-Zehnder modulator," *Nature Photon.*, vol. 11, pp. 482–485, Jul. 2017, doi: 10.1038/nphoton.2017.120.

[21] M. Takenaka *et al.*, "III–V/Si hybrid MOS optical phase shifter for Si photonic integrated circuits," *J. Lightw. Technol.*, vol. 37, no. 5, pp. 1474–1483, Mar. 2019, doi: 10.1109/jlt.2019.2892752.

[22] S. Menezo *et al.*, "High-speed heterogeneous InP-on-Si capacitive phase modulators," in *Proc. Opt. Fiber Commun. Conf.*, San Diego, CA, USA, Mar. 2018, Paper Tu3K.4., doi: 10.1364/OFC.2018.Tu3K.4.

[23] D.-M. Geum *et al.*, "Ultra-high-throughput production of III-V/Si wafer for electronic and photonic applications," *Sci. Rep.*, vol. 6, Feb. 2016, Art. no. 20610, doi: 10.1038/srep20610.(2016).

[24] D. Botteldooren and R. Baets, "Influence of band-gap shrinkage on the carrier-induced refractive index change in InGaAsP," *Appl. Phys. Lett.*, vol. 54, no. 20, pp. 1989–1991, May 1989, doi: 10.1063/1.101191.

[25] B. Bennett, R. Soref, and J. Del Alamo, "Carrier-induced change in refractive index of InP, GaAs and InGaAsP," *IEEE J. Quantum Electron.*, vol. 26, no. 1, pp. 113–122, Jan. 1990, doi: 10.1109/3.44924.

[26] J.-P. Weber, "Optimization of the carrier-induced effective index change in InGaAsP waveguides-application to tunable Bragg filters," *IEEE J. Quantum Electron.*, vol. 30, no. 8, pp. 1801–1816, Aug. 1994, doi: 10.1109/3.301645.

[27] M. Sotoodeh, A. H. Khalid, and A. A. Rezazadeh, "Empirical low-field mobility model for III–V compounds applicable in device simulation codes," *J. Appl. Phys.*, vol. 87, no. 6, pp. 2890–2900, Mar. 2000, doi: 10.1063/1.372274.

[28] S. Kim *et al.*, "Fabrication and characterization of single junction GaAs solar cell epitaxially grown on Si substrate," *Current Appl. Phys.*, vol. 15, pp. S40–S43, Sep. 2015, doi: 10.1016/j.cap.2015.04.022.

[29] B. Kunert, Y. Mols, M. Baryshniskova, N. Waldron, A. Schulze, and R. Langer, "How to control defect formation in monolithic III/V hetero-epitaxy on (100) Si? A critical review on current approaches," *Semicond. Sci. Technol.*, vol. 33, no. 9, Sep. 2018, Art. no. 093002, doi: 10.1088/1361-6641/aad655.

[30] J. Kwoen, B. Jang, J. Lee, T. Kageyama, K. Watanabe, and Y. Arakawa, "All MBE grown InAs/GaAs quantum dot lasers on on-axis Si (001)," *Opt. Express*, vol. 26, no. 9, pp. 11568–11576, Apr. 2018, doi: 10.1364/oe.26.011568.

[31] C. L. Andre, D. M. Wilt, A. J. Pitera, M. L. Lee, E. A. Fitzgerald, and S. A. Ringel, "Impact of dislocation densities on n+/p and p+/n junction GaAs diodes and solar cells on SiGe virtual substrates," *J. Appl. Phys.*, vol. 98, no. 1, Jul. 2005, Art. no. 014502, doi: 10.1063/1.1946194.

[32] Y. Kim, S.-H. Kim, Y. Ban, D. Yudistira, M. Pantouvaki, and J. V. Campenhout, "Proposal and simulation of a low loss, highly efficient monolithic III-V/Si optical phase shifter," *Group IV Photon.*, Singapore, Aug. 2019, Paper WP29, pp. 1–2.

[33] Q. Li *et al.*, "1.3 μm InAs quantum-dot micro-disk lasers on V-groove patterned and unpatterned (001) silicon," *Opt. Express*, vol. 24, no. 18, pp. 21038–21045, Sep. 2016, doi: 10.1364/oe.24.021038.

[34] Y. Mols *et al.*, "Structural analysis and resistivity measurements of InAs and GaSb fins on 300 mm Si for vertical (T)FET," *J. Appl. Phys.*, vol. 125, no. 24, Jun. 2019, Art. no. 245107, doi: 10.1063/1.5096015.

[35] H. Kim *et al.*, "Enhanced open-circuit voltage of InAs/GaAs quantum dot solar cells by hydrogen plasma treatment," *J. Vac. Sci. Technol. B, Nanotechnol. Microelectron., Mater., Process., Meas.*, vol. 33, no. 4, Jul. 2015, Art. no. 041401, doi: 10.1116/1.4926630.

[36] K. C. Hsieh, M. S. Feng, G. E. Stillman, N. Holonyak, C. R. Ito, and M. Feng, "Hydrogenation and subsequent hydrogen annealing of GaAs on Si," *Appl. Phys. Lett.*, vol. 54, no. 4, pp. 341–343, Jan. 1989, doi: 10.1063/1.100963.

Sanghyeon Kim (Member, IEEE) received the B.S., M.S., and Ph.D. degrees in electronic engineering from The University of Tokyo, Japan, in 2009, 2011, and 2014, respectively. After his Ph.D., he was with the Korea Institute of Science and Technology (KIST), South Korea, in 2014, until he moved to the Korea Advanced Institute of Science and Technology (KAIST), South Korea, in 2019. Before joining KAIST, he held a Post-Doctoral position at the IMEC Belgium, from 2017 to 2018. He is currently an Assistant Professor with the School of Electrical Engineering, KAIST. His current research interests include next-generation computing devices, monolithic 3D integration, MicroLED, thin-film imager, and MID-IR photonics.

Younghyun Kim (Member, IEEE) received the B.S. degree in electrical and electronic engineering from The University of Tokushima, Tokushima, Japan, in 2010, and the M.S. and Ph.D. degrees from The University of Tokyo, Tokyo, Japan, in 2012 and 2015, respectively. He is currently an Research and Development Engineer with the IMEC Belgium.

Yoojin Ban received the B.S. and M.S. degrees in electrical and electronic engineering from Yonsei University, South Korea, in 2013 and 2015, respectively. She joined the IMEC Belgium, as a Staff Research and Development Engineer. She is currently working on an optical modulator and circuit for Si photonics.

Marianna Pantouvaki received the Ph.D. degree in electronic engineering from University College London (UCL), U.K., in 2004. From 2003 to 2006, she was a Research Fellow with the Ultra-Fast Photonics Group, UCL, while she also spends one year as a Visiting Researcher at the Centre for Integrated Photonics, U.K., focusing on the monolithic integration of InP-based DBR lasers and modulators. From 2006 to 2010, she was a Back-End-Of-Line Integration Engineer for the Nano-interconnect Program at the IMEC. She through her activities at the imec has gained wide experience in the advanced CMOS process, strong expertise in nanofabrication of SOI-integrated lasers. She is currently responsible for the novel material and device exploration for optical interconnects at the IMEC.

Joris Van Campenhout received the Ph.D. degree in electrical engineering from Ghent University, Belgium, in 2007, for his work on hybrid integration of electrically driven III-V microdisk lasers on silicon photonic waveguide circuits. After the Ph.D., he joined the TJ Watson Research Center, IBM, USA, as a Post-Doctoral Researcher, where he developed silicon electro-optic switches for chip-level reconfigurable optical networks. He is currently the Chief Technologist Silicon Photonics and Program Director of the Optical I/O industry-affiliation R&D program at the IMEC. which targets the development of a scalable and industrially viable short-reach optical interconnect technology based on silicon photonics.